A Cell Transmission Model for Heterogeneous Multiclass Traffic Flow With Creeping

Shimao Fan
Coordinated Science Laboratory
University of Illinois at Urbana-Champaign
shimao@illinois.edu

Dan Work (corresponding author)
Department of Civil and Environmental Engineering and Coordinated Science Laboratory
University of Illinois at Urbana-Champaign
dbwork@illinois.edu

4437 words + 3 figures (250 words each) + 1 table (250 words each)

Total: 5437

ABSTRACT
A heterogeneous traffic model with creeping is developed as a multiclass generalization of the cell transmission model. Creeping occurs when small vehicles continue to advance in congestion even though larger vehicles have completely stopped. To capture creeping, the model is posed as a phase transition model which applies a multiclass cell transmission model in the non-creeping phase, and a classical scalar cell transmission model in the creeping phase. The discrete model with creeping is presented by considering the sending and receiving of vehicles for each vehicle class. Numerical tests are carried out to illustrate the creeping phenomenon, and a comparison with two exiting heterogeneous multiclass models is performed. The model can be used to study the evolution of traffic flow in many emerging economies, where significant creeping is observable.

INTRODUCTION

In this work, a new heterogeneous multiclass traffic flow model is introduced to capture the *creeping* phenomenon for traffic flow that involves vehicles which are highly heterogeneous in size. One observes that at a certain level of congestion, larger vehicles such as cars completely stop, while small vehicles such as motorbikes continue to move through the gaps between the large vehicles. This feature is called creeping, and is prevalent in the traffic flow of many emerging economies. It is desirable to develop heterogeneous models to study the key features of this kind of flow, and then apply these models to improve the severe traffic problems pervasive emerging economies (see the IBM Commuter Pain Index [1]).

To model distinct behaviors of different vehicle classes, a system of conservation laws model (fluid dynamics traffic model) is considered that has a general framework

$$\begin{aligned} \left(\rho_j\right)_t + \left(\rho_j v_j\right)_x = 0, \qquad & j = 1, \cdots, n, \\ v_j = V_j\left(\vec{\rho}\right), \quad \text{with} \quad & \vec{\rho} = \left(\rho_1, \cdots, \rho_n\right), \end{aligned} \tag{1}$$

which describes the conservation of vehicles for n vehicle classes indexed by j. Here, $\rho_j = \rho_j(x,t)$ is the traffic density of the jth class, which depends on both the location x and time t, and $V_j(\cdot)$ is the corresponding velocity function, which is a function of the density of each class. In the special case when $n = 1$, the system becomes the *Lighthill–Whitham–Richards* (LWR) model [2, 3], and the flux function $Q(\rho) = \rho V(\rho)$ is a *fundamental diagram* (e.g., [4, 5]). Thus, the model (1) can be interpreted as a multiclass extension of the LWR model.

The LWR model can be discretized resulting in the *cell transmission model* (CTM) [6], which is consistent with the well known Godunov scheme [7], as shown by Lebacque [8]. The CTM provides a way to construct a discrete solution to a scalar conservation law and it has a clear physical interpretation. The existing models for multiclass traffic flow that fit into framework (1) can be classified based on their assumptions on the interaction rules of different vehicle classes characterized by the specific form of the velocity functions $V_j(\cdot)$ (see Table 1). Depending on the definition of velocity function, the properties of *overtaking* and creeping (i.e., a specific type of overtaking when one vehicle class is stopped) can be investigated.

Homogeneous Multiclass Models

When all velocity functions are identical, i.e., $v_j = V(\vec{\rho})$, (1) is a *homogeneous multiclass model* since all vehicle classes follow the same kinematic behavior. An example of a homogeneous multiclass model is the *Logghe and Immers* model [9], which relates different vehicle classes by a scaling factor known as a *passenger car equivalent* (PCE), and the velocity function depends on a weighted sum of the densities of all vehicle classes called the *effective density*, i.e., $v_j = V\left(\sum_i \beta_i \rho_i\right)$, where β_i is the PCE applied to the ith class. Moreover, Zhang and Jin's model [11] and the 1-pipe special lane model by Daganzo [10] also fit into this category. A primary limitation of homogeneous models is that they do not allow one vehicle class to overtake another [16], and they are not appropriate to capture creeping. Thus, making distinctions in the velocity function among different vehicle classes is necessary in order to model overtaking behavior including creeping.

Heterogeneous Multiclass Models

Heterogeneous multiclass models are developed by distinguishing $V_j(\cdot)$ for each vehicle class. The model by Ngoduy and Liu [12] and the *Fastlane* model [13] characterize vehicle classes by their

	Model	Velocity v_j	Overtaking	Creeping
Homogeneous	Logghe & Immers [9]	$v_j = V\left(\sum_i \beta_i \rho_i\right)$	no	no
	Daganzo [10]	$v_j = V\left(\sum_i \rho_i\right)$	no	no
	Zhang & Jin [11]	$v_j = V\left(\rho_1, \rho_2\right)$	no	no
Heterogeneous	Ngoduy & Liu [12]	$v_j = V_j\left(\beta_j \sum_i \rho_i\right)$ with $v_j = V$ in congestion	freeflow	no
	Fastlane [13]	$v_j = V_j\left(\sum_i \beta_i \rho_i\right)$, with $v_j = V$ in congestion	freeflow	no
	Wong & Wong [14]	$v_j = V_j\left(\sum_i \rho_i\right)$	yes	no
	Zhu et al. [15]	$v_j = v_j^{\mathrm{m}} V\left(\sum_i \rho_i\right)$	yes	no
	n–populations [16]	$v_j = v_j^{\mathrm{m}} V\left(\sum_i \ell_i \rho_i\right)$	yes	no
	Nair et al. [17]	$v_j = pV_{\mathrm{c}}(s) + (1-p)V_{\mathrm{f}}(s)$, $p = \int_0^{s_j} g(s)ds$, $g(s)$ is distribution of s	yes	yes
	Creeping model [18]	$v_j = V_j\left(\sum_i \ell_i \rho_i\right)$, with $V_j(0) = v^{\mathrm{m}}$	yes	yes

TABLE 1 : *Classification of multiclass models according to the definition of velocity functions.*

maximum velocities, and assume the same function in congestion. As a consequence, the Ngoduy and Liu and Fastlane models allow overtaking in the freeflow regime, but not in congestion. Wong and Wong [14] introduced a simplified heterogeneous multiclass model of the form (1) that admits overtaking in freeflow and congestion. The velocity function of each class is a function of the *total density* (e.g. $v_j = V_j\left(\sum_i \rho_i\right)$) and they are distinct except at the jam density. Later, Benzoni–Gavage and Colombo [16] introduced the *n–populations model*, which extended Wong and Wong's model by explicitly taking the size of each vehicle class into account. Instead of explicitly conserving the number of vehicles, the system expresses conservation of the space occupied by each vehicle class. Consequently, the velocity function depends on the *total occupied space* $r = \sum_j \ell_j \rho_j$, i.e., $v_j = V_j(r)$. As presented in [16], by substituting $\hat{\rho}_j := \ell_j \rho_j$ in the n–populations model, both n–populations model and Wong and Wong's model fit into the same mathematical framework

$$\begin{aligned} \left(\hat{\rho}_j\right)_t + \left(\hat{\rho}_j v_j\right)_x = 0, \qquad & j = 1, \cdots, n, \\ v_j = V_j(r), \quad \text{with} \quad & r = \sum_{j=1}^{n} \hat{\rho}_j, \end{aligned} \tag{2}$$

where $\hat{\rho}_j$ is the space occupied by the jth class. These models suppose all vehicle classes either never stop (see [14]), or stop at a common *maximum occupied space* r^{m} (or equivalently an *effective jam density*) (e.g., [12, 13, 16]), i.e., $V_j(r^{\mathrm{m}}) = 0$, $j = 1, \cdots, n$. Thus, they are not appropriate to model the creeping feature.

A heterogeneous multiclass model that allows for creeping is proposed by Nair et al. [17], and is known as the *porous model*. In this model, the velocity of each vehicle class is determined

by the availability of empty spaces s (pores). Letting s_j represent a critical pore size for the jth class, vehicles may be in freeflow ($s \geq s_j$) or get restricted ($s < s_j$) with velocity functions $V_{\mathrm{f}}(\cdot)$ and $V_{\mathrm{c}}(\cdot)$, respectively. The velocity of the jth class is

$$v_j = V_j(s) = \left(\int_{s_j}^{\infty} g(\omega)d\omega\right) V_{\mathrm{f}}(s) + \left(\int_0^{s_j} g(\omega)d\omega\right) V_{\mathrm{r}}(s), \tag{3}$$

where $g(\cdot)$ is the probability density function of the pores sizes for a given time. The creeping property is shown by numerical simulations, but significant analytical results are missing due to the complexity of the model (3), e.g., the density function $g(\cdot)$ evolves with time.

Recently, a simplified two class *creeping model* was proposed by Fan and Work [18] under the framework (2) in terms of occupied space, which distinguishes the maximum occupied space r^{m} in each vehicle class. By allowing r^{m} to vary between vehicle classes, the creeping phenomenon can be captured. Moreover, the well-posedness of the creeping model is proved, which is an important property that has not been established for many heterogeneous models due to the complexity of the resulting system of conservation laws (e.g., [16, 19]). Due to the challenge in constructing a solution to the creeping model in an analytical approach (e.g., construction of a Riemann solver), and the need for discrete models for many practical control and estimation applications, it is desirable to construct a discrete form of the creeping model.

Outline and Contributions

The main contributions of this article include three aspects: (*i*) a discrete two class heterogeneous model that allows creeping is introduced; (*ii*) a systematic approach to extend the CTM to heterogeneous multiclass models is proposed, which supports discrete implementations of the n-populations and creeping models, as well as a simplified variant of the porous model; and (*iii*) the features of the creeping model are validated by numerical simulations, and comparisons with respect to the n–populations model and the porous model are performed.

The remainder of article is organized as follows. In Section 2, the creeping model for two vehicle classes is outlined. Next, a discrete formulation of the creeping model is proposed in Section 3. Section 4 is devoted to validate the features of the proposed model by performing numerical simulations and comparing to the n–populations model and the porous model.

A TWO CLASS HETEROGENEOUS MODEL WITH CREEPING

First, the main features of the creeping model [18] are outlined. The model is posed as a *phase transition model* [20, 21] that considers two phases: a *non-creeping phase* and a *creeping phase*, which are defined as follows:

$$\begin{aligned} \mathscr{D}_1 &= \left\{(\rho_1,\rho_2) \in \mathbb{R}^2 \mid \rho_j \geq 0,\ j = 1,2;\ 0 < \rho_1 + \rho_2 \leq r_2^{\mathrm{m}}\right\}, \\ \mathscr{D}_2 &= \left\{(\rho_1,\rho_2) \in \mathbb{R}^2 \mid 0 \leq \rho_2 \leq r_2^{\mathrm{m}};\ r_2^{\mathrm{m}} \leq \rho_1 + \rho_2 \leq r_1^{\mathrm{m}}\right\}, \end{aligned} \tag{4}$$

where ρ_j and r_j^{m} represent the occupied space and the maximum occupied space of the jth class. The domain $\mathscr{D}$ of the model (6) is defined as a union of $\mathscr{D}_1$ and $\mathscr{D}_2$:

$$\mathscr{D} = \left\{(\rho_1,\rho_2) \in \mathbb{R}^2 \mid 0 \leq \rho_j \leq r_j^{\mathrm{m}},\ j = 1,2;\ 0 < \rho_1 + \rho_2 \leq r_1^{\mathrm{m}}\right\}, \tag{5}$$

which has a trapezoidal shape (see Figure 1(b)).

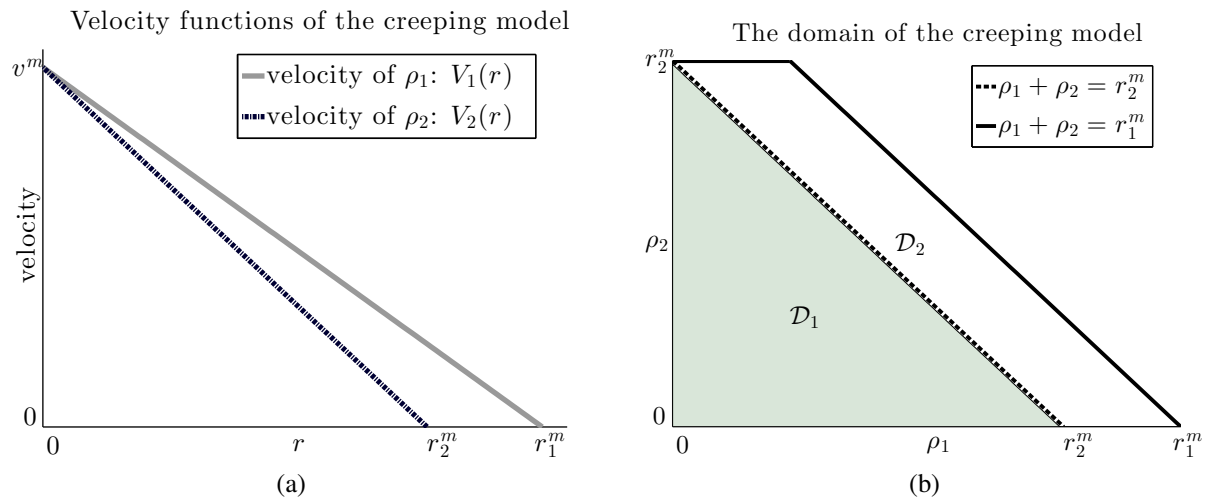

FIGURE 1 : *(a) Velocity functions of the creeping model (9). Here, the solid-gray line represents the velocity of the first vehicle class, and the dashed-blue line is the velocity of the second vehicle class. (b) The domain of the creeping model (9).*

In $\mathscr{D}_1$, the model is a system of conservation laws, where the dynamics of both vehicle classes can be studied. In $\mathscr{D}_2$, the large vehicles are stationary at a time t, and thus the density remains unchanged, i.e., $(\rho_2)_t = 0$. In this case, the system reduces to the LWR model for ρ_1 with possibility of discontinuous fluxes in space, which correspond to shock profiles of ρ_2. Thus, $\mathscr{D}_2$ represents a creeping phase, and $\mathscr{D}_1$ is a non-creeping phase (see Figure 1(b)). The model is written as

$$\begin{cases} \begin{cases} (\rho_1)_t + \big(\rho_1 V_1(r)\big)_x &= 0, \\ (\rho_2)_t + \big(\rho_2 V_2(r)\big)_x &= 0, \end{cases} & \text{if} \quad (\rho_1,\rho_2) \in \mathscr{D}_1, \\ \\ \begin{cases} (\rho_1)_t + \big(\rho_1 V_1(r)\big)_x &= 0, \\ \text{with} \quad (\rho_2)_t &= 0, \end{cases} & \text{if} \quad (\rho_1,\rho_2) \in \mathscr{D}_2, \end{cases} \tag{6}$$

where a phase change is defined between $\mathscr{D}_1$ and $\mathscr{D}_2$.

Here, the velocity functions $V_j(\cdot)$, $j = 1,2$ have the following properties:

$$V_j'(r) < 0, \quad V_j(0) = v^{\mathrm{m}}, \quad V_1(r_1^{\mathrm{m}}) = V_2(r_2^{\mathrm{m}}) = 0, \quad r_2^{\mathrm{m}} < r_1^{\mathrm{m}} < 2r_2^{\mathrm{m}}. \tag{7}$$

It is assumed that the velocity functions are strictly decreasing, and both vehicle classes possess a common maximal speed v^{m} (see Figure 1(a)). The latter assumption is valid when the maximum velocities of different vehicle classes are restricted by a speed limit achievable by both classes. Moreover, the condition $r_1^{\mathrm{m}} < 2r_2^{\mathrm{m}}$ is a realistic condition on the maximum occupied space.

Based on the assumptions in the velocity function (7), one may propose various velocity functions to generate multiclass fundamental diagrams, such as Drake's exponential model, the smooth three-parameter model [22], or the Greenshields model [4]. For mathematical simplicity, the linear Greenshields model is used in this work:

$$V_1(r) = v^{\mathrm{m}}(1 - r/r_1^{\mathrm{m}}), \qquad V_2(r) = v^{\mathrm{m}}(1 - r/r_2^{\mathrm{m}}). \tag{8}$$

The model (6) with Greenshields velocity functions (8) is written as

$$\begin{cases} \begin{cases} (\rho_1)_t + \left(\rho_1 v^{\mathrm{m}}(1-(\rho_1+\rho_2)/r_1^{\mathrm{m}})\right)_x &= 0, \\ (\rho_2)_t + \left(\rho_2 v^{\mathrm{m}}(1-(\rho_1+\rho_2)/r_2^{\mathrm{m}})\right)_x &= 0, \end{cases} & \text{if} \quad (\rho_1,\rho_2) \in \mathscr{D}_1, \\ \\ \begin{cases} (\rho_1)_t + \left(\rho_1 v^{\mathrm{m}}(1-(\rho_1+\rho_2)/r_1^{\mathrm{m}})\right)_x &= 0, \\ \text{with} \quad (\rho_2)_t &= 0, \end{cases} & \text{if} \quad (\rho_1,\rho_2) \in \mathscr{D}_2. \end{cases} \tag{9}$$

Remark 1. The phase transition models apply a scalar conservation law in freeflow, and a system of conservation laws in congestion. In the creeping model (9), a scalar model is employed in the creeping phase, and a system of conservation laws is applied in the non-creeping phase.

By observing Figure 1(a), the deviation between the two velocity functions strictly increases with r by using the linear velocity functions. Alternative velocity functions may be considered to provide more control over the deviations and to potentially improve the predictive capabilities of the model. Moreover, one sees that the Greenshields model (8) generates a negative velocity for the second vehicle class for $r > r_2^{\mathrm{m}}$. The creeping model (9) successfully excludes the presence of this nonphysical negative velocity by applying a phase transition.

Remark 2. Another approach one may consider to avoid negative velocity in the second vehicle class while avoiding the need to pose the creeping model as a phase transition model is to redefine the velocity function as

$$\tilde{V}_2(r) = \begin{cases} V_2(r), & \text{if} \quad r \le r_2^{\mathrm{m}}, \\ 0, & \text{if} \quad r_2^{\mathrm{m}} < r \le r_1^{\mathrm{m}}. \end{cases} \tag{10}$$

This approach is penalized by the loss of strict hyperbolicity for $r > r_2^{\mathrm{m}}$ [18].

In summary, the creeping model (9) is a phase transition model, where phase changes are defined between two domains, $\mathscr{D}_1$ and $\mathscr{D}_2$. As presented in [18], the existence of a solution to the model can be shown in a general approach that includes verifying the strict hyperbolicity of the model, investigating the elementary waves and using them to construct a Riemann solver, and proving the existence of a solution following Glimm's random choice method [23, 24] and the wavefront tracking algorithm [25, 26]. Next, a discrete formulation of the creeping model is introduced.

A CELL TRANSMISSION MODEL WITH CREEPING

In this section, a cell transmission model with creeping is developed based on a discrete formulation of the continuum creeping model (9). The model can be seen as a multiclass extension of the CTM.

The Scalar Cell Transmission Model

The CTM discretizes space into cells with size Δx, and computes the density in each cell by examining its inflow and outflow over the time interval Δt. Here, three adjacent cells ($i-1$, i and $i+1$) are considered with constant initial densities ρ_{i-1}^k, ρ_i^k, and ρ_{i+1}^k at the time $t = k\Delta t$, and the evolution of traffic density in the cell i is studied. The key elements of the CTM are listed as follows.

1. The evolution equation describes conservation of vehicles via discretization of the LWR model with a Godunov scheme:

$$\rho_i^{k+1} = \rho_i^k + \frac{\Delta t}{\Delta x}\left(F_{i-1/2}^k - F_{i+1/2}^k\right), \tag{11}$$

where ρ_i^{k+1} is the traffic density of the ith cell at the next time step $t = (k+1)\Delta t$, and $F_{i-1/2}^k$ and $F_{i+1/2}^k$ are the inflow and outflow of the cell i at the current time $t = k\Delta t$. By rearranging (11) into

$$\left(\rho_i^{k+1} - \rho_i^k\right)\Delta x = \left(F_{i-1/2}^k - F_{i+1/2}^k\right)\Delta t, \tag{12}$$

the scheme explicitly describes the conservation of vehicles, where the change in vehicles at the cell i during time interval Δt (the left side of (12)) is exactly equal to the difference between the vehicles entering from the upstream cell boundary and the vehicles exiting the downstream cell boundary (the right side of (12)).

2. The inflow and outflow $F_{i-1/2}^k$ and $F_{i+1/2}^k$ are determined by the minimum of the vehicles available to be sent from the upstream cell, and the availability of the downstream cell to receive vehicles:

$$F_{i-1/2}^k = \min\left\{S(\rho_{i-1}^k)\ ,\ R(\rho_i^k)\right\}\ , \qquad F_{i+1/2}^k = \min\left\{S(\rho_i^k)\ ,\ R(\rho_{i+1}^k)\right\}, \tag{13}$$

where $S(\cdot)$ and $R(\cdot)$ are known as the sending and receiving functions.

3. The sending and receiving functions are defined based on the flux function $Q(\rho)$:

$$S(\rho) = \begin{cases} Q(\rho), & \text{if} \quad \rho \le \rho_c, \\ Q_{\max}, & \text{if} \quad \rho > \rho_c, \end{cases} \qquad R(\rho) = \begin{cases} Q_{\max}, & \text{if} \quad \rho \le \rho_c, \\ Q(\rho), & \text{if} \quad \rho > \rho_c, \end{cases} \tag{14}$$

where ρ_c denotes the critical density where $Q_{\max}$ is obtained. One sees that $S(\cdot)$ gives the maximum possible flow that can be sent from the upstream cell given the upstream density, and $R(\cdot)$ defines the maximum flow that can be received in the downstream cell given the downstream density.

Discrete Formulation of Multiclass Traffic Flow Models

Recall that multiclass traffic model (1) generalizes the LWR model to multiclass traffic flow, and thus the CTM can also be generalized to its multiclass equivalent by mass conservation of each vehicle class, which has the following form

$$\left(\rho_{j,i}^{k+1} - \rho_{j,i}^k\right)\Delta x = \left(F_{j,i-1/2}^k - F_{j,i+1/2}^k\right)\Delta t, \qquad j = 1, \cdots, n, \tag{15}$$

where $\rho_{j,i}^{k+1}$ and $\rho_{j,i}^k$ are traffic densities in the jth vehicle class of the cell i at the time $t = (k+1)\Delta t$ and $t = k\Delta t$, respectively, and $F_{j,i-1/2}^k$ and $F_{j,i+1/2}^k$ are the inflow and outflow of the vehicle class. These fluxes are obtained by explicitly analyzing the sending and receiving potential for each vehicle class, similar to the CTM. One sees that (15) expresses the conservation of vehicles of each vehicle class in each cell. Next, the inflow and outflow functions are defined.

The flow of the jth vehicle class is the minimum of sending and receiving functions of the class. For simplicity, the initial states of upstream and downstream cells are represented as $u^- = (\rho_1^-, \cdots, \rho_n^-)$ and $u^+ = (\rho_1^+, \cdots, \rho_n^+)$, which are vectors of densities of all vehicle classes. The flow of the jth vehicle classes across the cell interface is determined as

$$F_j = \min\left\{S_j(\rho_1^-, \cdots, \rho_n^-),\ R_j(\rho_1^+, \cdots, \rho_n^+)\right\}, \qquad j = 1, \cdots, n, \tag{16}$$

where $S_j(\cdot)$ and $R_j(\cdot)$ represent the sending and receiving functions of the vehicle class indexed by j, which are functions of each vehicle class.

In the n–populations model (2), the flow (16) can be simplified to

$$F_j = \min\left\{S_j(\rho_j^-, r^-),\ R_j(\rho_j^+, r^+)\right\}, \quad r^- = \sum_{j=1}^{n} \rho_j^-, \quad r^+ = \sum_{j=1}^{n} \rho_j^+. \tag{17}$$

It is noted that $S_j(\cdot)$ and $R_j(\cdot)$ depend on the initial traffic densities of the jth vehicle class ρ_j^- and ρ_j^+, and the free space remaining for the vehicle class, which can be computed from r^- and r^+. The sending and receiving functions are defined as follows:

$$\begin{aligned} S_j(\rho_j^-, r^-) &= \begin{cases} Q_j(\rho_j^-, r^-), & \text{if} \quad \rho_j^- \le \rho_j^{\mathrm{c}}, \\ Q_j^{\max}, & \text{if} \quad \rho_j^- > \rho_j^{\mathrm{c}}, \end{cases} \quad j = 1, \cdots, n, \\ R_j(\rho_j^+, r^+) &= \begin{cases} Q_j^{\max}, & \text{if} \quad \rho_j^+ \le \rho_j^{\mathrm{c}}, \\ Q_j(\rho_j^+, r^+), & \text{if} \quad \rho_j^+ > \rho_j^{\mathrm{c}}, \end{cases} \quad j = 1, \cdots, n, \end{aligned} \tag{18}$$

where $Q_j(\rho_j, r) = \rho_j V_j(r)$ is the flux function of the jth class, and ρ_j^{c} denotes the critical density such that $Q_j(\rho_j, r)$ is maximized for a given initial state, represented by $Q_j^{\max}$. Letting $V_j(\cdot)$ be the Greenshields model in the n–populations model, one can calculate ρ_j^{c} function explicitly as

$$\rho_j^{\mathrm{c}} = \frac{r^{\mathrm{m}} - \sum_{i \neq j} \rho_i}{2}, \tag{19}$$

where r^{m} is the common maximum occupied space for all vehicle classes.

A Two Class Cell Transmission Model with Creeping

Based on (15) and (9), the creeping CTM is posed, where the updating rules of the traffic densities of both vehicle classes in the cell i are given as

$$\begin{cases} \begin{cases} \left(\rho_{1,i}^{k+1} - \rho_{1,i}^{k}\right)\Delta x &= \left(F_{1,i-1/2}^{k} - F_{1,i+1/2}^{k}\right)\Delta t, \\ \left(\rho_{2,i}^{k+1} - \rho_{2,i}^{k}\right)\Delta x &= \left(F_{2,i-1/2}^{k} - F_{2,i+1/2}^{k}\right)\Delta t, \end{cases} & \text{if} \quad (\rho_{1,i}^{k}, \rho_{2,i}^{k}) \in \mathscr{D}_1, \\ \begin{cases} \left(\rho_{1,i}^{k+1} - \rho_{1,i}^{k}\right)\Delta x &= \left(F_{1,i-1/2}^{k} - F_{1,i+1/2}^{k}\right)\Delta t, \\ \text{with} \quad \rho_{2,i}^{k+1} &= \rho_{2,i}^{k}, \end{cases} & \text{if} \quad (\rho_{1,i}^{k}, \rho_{2,i}^{k}) \in \mathscr{D}_2. \end{cases} \tag{20}$$

In $\mathscr{D}_1$, it is a system of CTMs illustrating the conservation of two vehicle classes. In $\mathscr{D}_2$, the classical CTM is used for the first vehicle class (with smaller size), and the density of the second vehicle class (with larger size) remains unchanged from the current time $t = k\Delta t$ to the next time step $t = (k+1)\Delta t$.

Similar as the CTM, the flow is determined by taking the minimum of the sending and receiving functions, which are studied in detail for each vehicle class. Here, two adjacent cells with initial states $u^- = (\rho_1^-, \rho_2^-)$ and $u^+ = (\rho_1^+, \rho_2^+)$ are considered.

Sending and Receiving Functions for the first vehicle class
The flux function of the first vehicle class is defined as

$$Q_1(\rho_1,\rho_2) = \rho_1 V_1(\rho_1+\rho_2), \qquad (\rho_1,\rho_2)\in\mathscr{D}, \tag{21}$$

where $V_1(\cdot)$ is the linear model defined in (8). Based on (18), the sending and receiving functions of the first vehicle class are defined in the domain $\mathscr{D}$ as:

$$\begin{aligned} S_1(\rho_1^-,\rho_2^-) &= \begin{cases} Q_1(\rho_1^-,\rho_2^-), & \text{if} \quad \rho_1^- \le \rho_1^{\mathrm{c}}(\rho_2^-), \\ Q_1^{\max}(\rho_2^-), & \text{if} \quad \rho_1^- > \rho_1^{\mathrm{c}}(\rho_2^-), \end{cases} \quad (\rho_1^-,\rho_2^-)\in\mathscr{D}, \\ R_1(\rho_1^+,\rho_2^+) &= \begin{cases} Q_1^{\max}(\rho_2^+), & \text{if} \quad \rho_1^+ \le \rho_1^{\mathrm{c}}(\rho_2^+), \\ Q_1(\rho_1^+,\rho_2^+), & \text{if} \quad \rho_1^+ > \rho_1^{\mathrm{c}}(\rho_2^+), \end{cases} \quad (\rho_1^+,\rho_2^+)\in\mathscr{D}, \end{aligned} \tag{22}$$

where $Q_1^{\max}(\rho_2) = \max_{\rho_1}\{Q_1(\rho_1,\rho_2)\}$ is the maximum of (21), and $\rho_1^{\mathrm{c}}(\rho_2) = \frac{r_1^{\mathrm{m}}-\rho_2}{2}$ is the critical density of ρ_1 such that $Q_1^{\max}$ is obtained. Here, $\rho_1^{\mathrm{c}}(\rho_2) > 0$ since $\rho_2 < r_1^{\mathrm{m}}$ based on the velocity definition (7) of the creeping model. Note that the maximum flow of ρ_1 is a function of ρ_2, i.e., the space occupied by the second vehicle class.

It can be shown that the definition (22) provides physically meaningful solutions of traffic flow of the first vehicle class. For instance, in the case when $\rho_1^- = 0$, i.e., no upstream vehicles of the first class are available to be sent, one checks that $S_1 = 0$, and therefore $F_1 = 0$. When the second vehicle class is absent, i.e., $\rho_2^- = 0$ and $\rho_2^+ = 0$, the sending and receiving functions (22) are consistent with those of the LWR model (14).

Sending and Receiving Functions for the second vehicle class
The flux function of the second vehicle class is

$$Q_2(\rho_1,\rho_2) = \rho_2 V_2(\rho_1+\rho_2), \qquad (\rho_1,\rho_2)\in\mathscr{D}_1, \tag{23}$$

where the velocity function $V_2(\cdot)$ is the linear model (8). Note that $Q_2(\cdot)$ is only defined for the non-creeping phase $\mathscr{D}_1$, in which both ρ_1 and ρ_2 evolve. The second vehicle class is stationary in the creeping phase, and its density remains constant (20). As a result, the sending and receiving functions for ρ_2 are only necessary in the non-creeping phase, and are given by:

$$\begin{aligned} S_2(\rho_1^-,\rho_2^-) &= \begin{cases} Q_2(\rho_1^-,\rho_2^-), & \text{if} \quad \rho_2^- \le \rho_2^{\mathrm{c}}(\rho_1^-), \\ Q_2^{\max}(\rho_1^-), & \text{if} \quad \rho_2^- > \rho_2^{\mathrm{c}}(\rho_1^-), \end{cases} \quad (\rho_1^-,\rho_2^-)\in\mathscr{D}_1, \\ R_2(\rho_1^+,\rho_2^+) &= \begin{cases} Q_2^{\max}(\rho_1^+), & \text{if} \quad \rho_2^+ \le \rho_2^{\mathrm{c}}(\rho_1^+), \\ Q_2(\rho_1^+,\rho_2^+), & \text{if} \quad \rho_2^+ > \rho_2^{\mathrm{c}}(\rho_1^+), \end{cases} \quad (\rho_1^+,\rho_2^+)\in\mathscr{D}_1, \end{aligned} \tag{24}$$

where $Q_2^{\max}(\rho_1) = \max_{\rho_2}\{Q_2(\rho_1,\rho_2)\}$, and $\rho_2^{\mathrm{c}}(\rho_1) = \frac{r_2^{\mathrm{m}}-\rho_1}{2}$ is the critical density of the second vehicle class such that $Q_2^{\max}$ is obtained. Here, the critical density is non-negative $\rho_2^{\mathrm{c}}(\rho_1) \ge 0$ in $\mathscr{D}_1$. Similar to (22), it can be checked that the flow of ρ_2 through a cell interface is physical meaningful based on the definition of (24). For instance, if $\rho_1^+ + \rho_2^+ = r_2^{\mathrm{m}}$, i.e., the case when the downstream cell has no room to receive ρ_2, one verifies that the flow of the second vehicle class vanishes.

A Discrete Porous Model

For the porous model, a Godunov scheme is presented [17], where the flow of each class is determined by explicitly by analyzing the available number of vehicles available to be sent from the upstream, and given rules how the vehicles compete for the free spaces at downstream, which defines the receiving function. In particular, a portion of free space is reserved for smaller vehicles exclusively when the size of pore is not large enough to accommodate large vehicles. The remaining space is shared by both vehicle classes.

As pointed out in [17], the scheme is distinct from the cell transmission type models because the distribution of pore spaces evolves with time. Recall the velocity function defined in (3), two velocity profiles $V_{\mathrm{f}}(\cdot)$ (freeflow) and $V_{\mathrm{r}}(\cdot)$ (restricted flow) are defined for each vehicle class

$$V_{\mathrm{f}}(s) = v_j^{\mathrm{m}} \left(1 - \int_0^{s_j} g(\omega) d\omega\right)^{\alpha_{\mathrm{f}}}, \quad V_{\mathrm{r}}(s) = v_j^{\mathrm{m}} \left(1 - \int_0^{s_j} g(\omega) d\omega\right)^{\alpha_{\mathrm{r}}}, \quad j = 1, \cdots, n, \tag{25}$$

where s_j is the critical pore size of the jth class with $\alpha_{\mathrm{f}} \leq \alpha_{\mathrm{r}}$, since $V_{\mathrm{f}} \geq V_{\mathrm{r}}$. Based on the velocity definition (3), the velocity function is not deterministic; it depends on the distribution of the pore size.

A discrete solver for the porous model fits into the framework of multiclass cell transmission models used in this work by making the following simplifications:

1. The density function of pore spaces is time invariant.

2. A common velocity function is defined for freeflow and restricted flow, i.e., $V_{\mathrm{f}} = V_{\mathrm{r}}$.

One sees that these assumptions render a fixed velocity density function, and thus the model is deterministic. A cell transmission model for the deterministic porous model with a uniform density function, i.e., $g(s) = \frac{1}{s_{\max}(r)}$ is presented next. Here, $s_{\max}(\cdot)$ is the maximum size of the pores, and is a function of the total occupied space r. In this case, the velocity function of the jth class is

$$v_j(r) = v_j^{\mathrm{m}} \left(1 - \frac{s_j}{s_{\max}(r)}\right), \quad r = \sum_j \rho_j, \quad j = 1, \cdots, n, \tag{26}$$

where s_j is the critical pore space of the jth class, and $s_{\max}(\cdot)$ is a decreasing function.

Next, the sending and receiving functions can be defined, similar as those of the n–populations model (18). Moreover, the critical density ρ_j^{c} is calculated for a given function $s_{\max}(\cdot)$. Finally, the flow of each class is determined by the taking the minimum of sending and receiving functions.

Remark 3. The two class discrete framework of the deterministic porous model is consistent with the creeping model by assigning a common maximum velocity $v_1^{\mathrm{m}} = v_2^{\mathrm{m}} = v^{\mathrm{m}}$, and choosing the function $s_{\max}(\cdot)$ as

$$s_{\max}(r) = \frac{c}{r}, \qquad r = \sum_j \rho_j. \tag{27}$$

where c is a constant model parameter.

Similar to the CTM, Δx and Δt are chosen to statisfy the CFL condition, $v^{\mathrm{m}} \frac{\Delta t}{\Delta x} \leq 1$, where v^{m} is the speed limit.

NUMERICAL SIMULATIONS AND COMPARISONS

This section is devoted to illustrate the overtaking and creeping properties of the creeping model (20) in numerical simulations, and compares it to the n–populations model [16] and the porous model [17] with two vehicle classes.

For these numerical tests, the following parameters are used for the creeping model:

$$v^{\mathrm{m}} = 1.5, \quad \text{and} \quad r_1^{\mathrm{m}} = 1.5, \quad r_2^{\mathrm{m}} = 1.0, \tag{28}$$

where v^{m} represent the speed limit, and r_1^{m} and r_2^{m} are the maximum occupied spaces of the two vehicle classes.

In the n–populations model, let

$$v_1^{\mathrm{m}} = 1.5, \quad v_2^{\mathrm{m}} = 1.0, \quad \text{and} \quad r^{\mathrm{m}} = 1.5. \tag{29}$$

Here, v_1^{m} and v_2^{m} are the maximum velocities of both vehicle classes, and r^{m} is the common maximum occupied space. Thus, the first vehicle class is assumed to move faster in both models.

Additional model parameters are necessary for the porous model. Here, the deterministic porous model with a specific choice of the $s_{\max}(\cdot)$ such as in [17] is considered. In particular,

$$s_{\max}(r) = \lambda e^{-cr}, \tag{30}$$

where $\lambda = 4.0$, and c is calculated such that the velocity is zero at the maximum occupied space, i.e., $c_j = \frac{\log \frac{\lambda}{s_j}}{r_j^{\mathrm{m}}}$, $j = 1,2$. The choice of r_j^{m} is the same as the creeping model. In the velocity function, let

$$\alpha_{\mathrm{f}} = \alpha_{\mathrm{r}} = 1.0, \qquad \text{and} \qquad v^{\mathrm{m}} = 1.5. \tag{31}$$

Moreover, the critical pore sizes are chosen as

$$s_1 = 1.0, \qquad s_2 = 2.0. \tag{32}$$

Again, the first vehicle class represents small and fast vehicles.

Furthermore, the computational domain is chosen as $x \in [0,50]$, with $\Delta x = 0.05$ and the time step Δt is chosen based on the CFL condition, letting

$$\Delta t = \Delta x / v^{\mathrm{m}}, \quad \text{where} \quad v^{\mathrm{m}} = \max\{v_1^{\mathrm{m}}, v_2^{\mathrm{m}}\}. \tag{33}$$

Example 1: Overtaking

In this test, the larger vehicle class ρ_2 begins in front of the smaller class ρ_1 at $t = 0$. The initial condition for both vehicle classes is given as follows:

$$\rho_1(x,0) = \begin{cases} 0.8, & \text{if} \quad x \in [1,10], \\ 0, & \text{otherwise}, \end{cases} \qquad \rho_2(x,0) = \begin{cases} 0.8, & \text{if} \quad x \in [11,50], \\ 0, & \text{otherwise}. \end{cases} \tag{34}$$

On the boundaries, assume the upstream inflow is zero, and vehicles are allowed to flow out of the study area freely, i.e., the region downstream of the study region is empty.

As time evolves, the first vehicle class overtakes the second class. At $t = 50$, all three models exhibit overtaking (see Figure 2), although the overtaking occurs at different times due to the structure of the three models. The main result of Example 1 is is that each of the three models allow one vehicle class to overtake another, which is not possible in homogeneous multiclass traffic flow models.

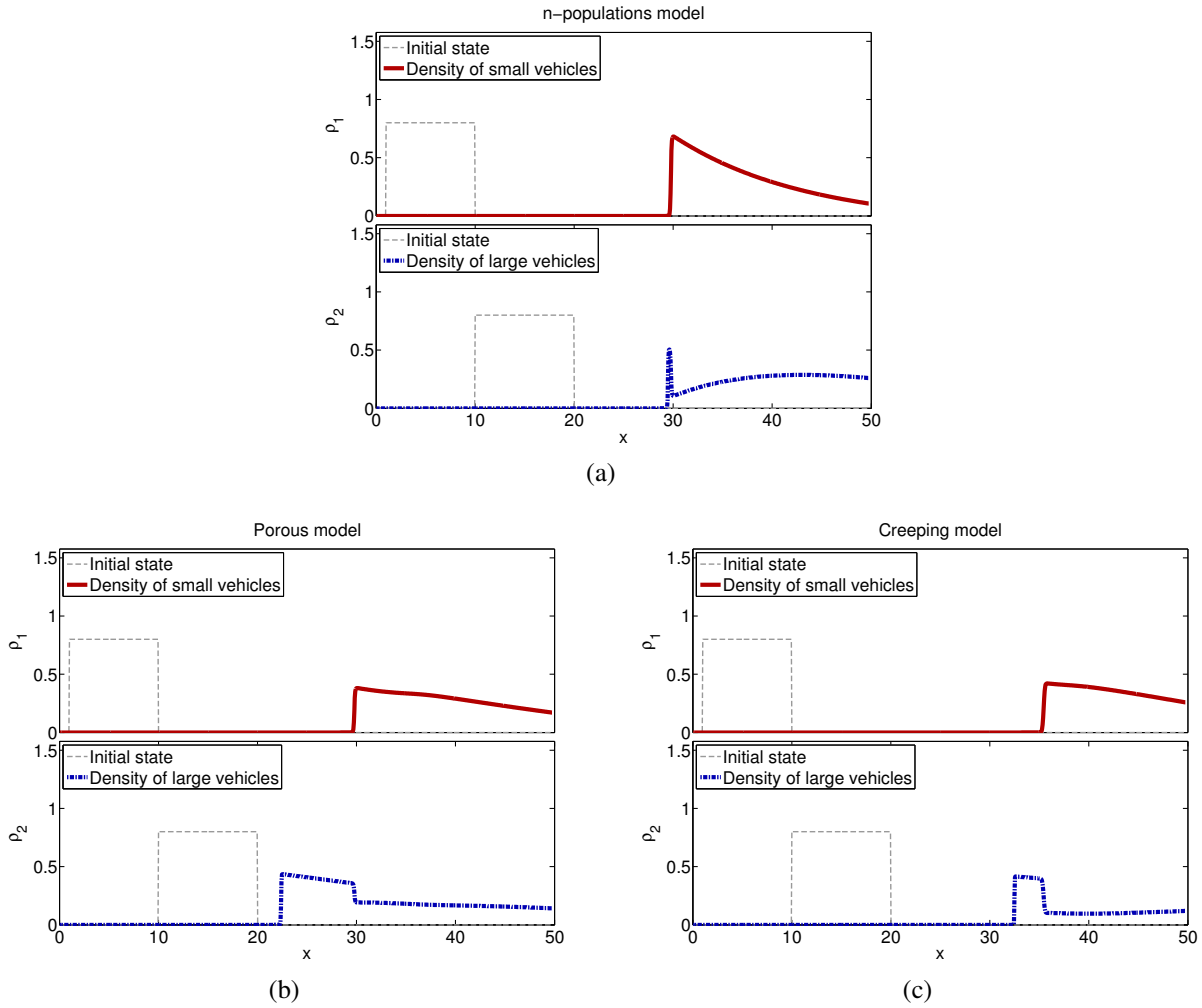

FIGURE 2 : *Example 1: an experiment of overtaking. (a) shows the simulation result of the n–populations model; (b) shows the simulation result of the porous model; and (c) shows the simulation result of the creeping model. In each figure, the densities of the first vehicle class (thick-solid-red) and the second vehicle class (thick-dashed-blue), together with the initial condition (thin-dashed-gray) are shown. All results are given at* $t = 50$.

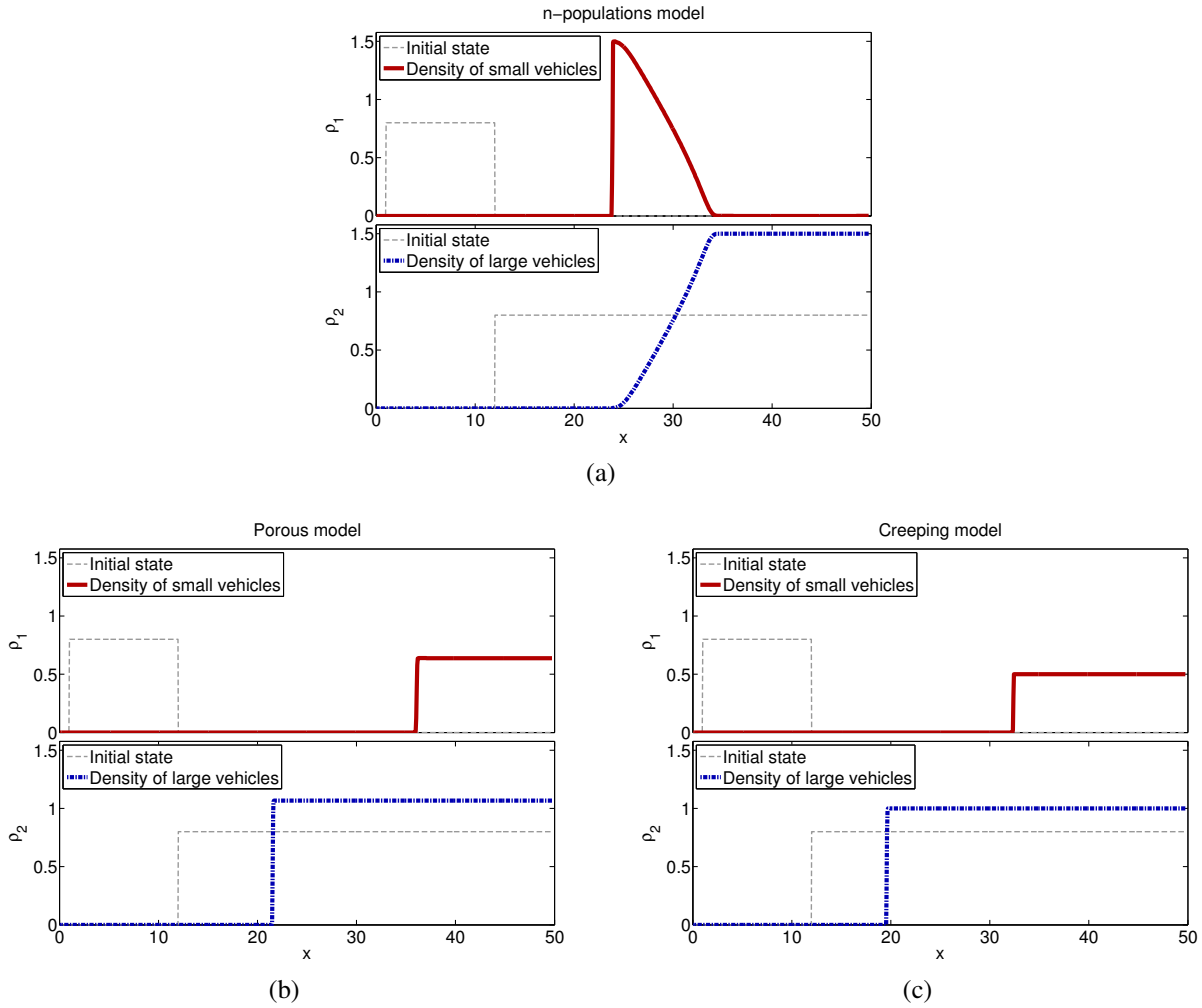

FIGURE 3 : *Example 2: an experiment of creeping. (a) shows the simulation result of the n–populations model; (b) shows the simulation result of the porous model; and (c) shows the simulation result of the creeping model. In each figure, the densities of the first vehicle class (thick-solid-red) and the second vehicle class (thick-dashed-blue), together with the initial condition (thin-dashed-gray) are shown. All results are given at* $t = 200$.

Example 2: Creeping
The next example depicts a scenario when two vehicle classes approach a red traffic light. Here, the same model parameters are applied as in the Example 1, but a new initial condition is given as follows:

$$\rho_1(x,0) = \begin{cases} 0.8, & \text{if } x \in [1,12], \\ 0, & \text{otherwise,} \end{cases} \qquad \rho_2(x,0) = \begin{cases} 0.8, & \text{if } x \in [13,50], \\ 0, & \text{otherwise.} \end{cases} \tag{35}$$

This initial condition describes a situation where the first vehicle class starts behind the second vehicle class. For the boundary condition, the inflow from upstream is zero and the downstream outflow for both vehicle classes is prescribed as zero to model a red traffic light. Example 2 is suitable to verify whether a model can capture creeping or not (see Figure 3).

Similar to the previous experiment, overtaking occurs in all models as time evolves, where the first vehicle class catches up and competes for free spaces with the second vehicle class. For the second vehicle class, shock waves are triggered from the right boundary and travel backwards into the computational domain. One observes that the second vehicle class accumulates at the traffic light.

At $t = 200$, one observes very different configurations of the density profiles between the n–populations model (see Figures 3(a)) and the other two models (see Figures 3(b), 3(c)). In the n–populations model, the road segment adjacent to the red traffic light $x \in [33,50]$ is occupied exclusively by larger vehicles, while traffic on the road segment $x \in [25,33]$ is composed by two vehicle classes. It is clear that the n–populations model does not allow creeping.

In the porous model and the creeping model, the first vehicle class with smaller size is able to overtake the second vehicle class even through the larger vehicles are stationary due to the red traffic light. At $t = 200$, both vehicle classes appear near the right boundary of the study area, and the smaller vehicle class creeps up to the front of the queue. This test shows that the creeping model is able to model creeping in a heterogeneous traffic flow, similar to the porous model. This result is not surprising by noting that the creeping model and the porous model implemented in the numerical simulation fit into the same framework of the CTM, and they can be rendered identical by adjusting the setting of the porous model (see Remark 3).

Discussion
Two experiments are performed to show the overtaking and creeping features of the three models: the n–populations model, the porous model, and the creeping model. Even though both the porous model and the creeping model allow creeping, one sees that the complexity of implementation for creeping model (20) is reduced compared to the porous model. This is not surprising, because porous model [17] provides a more general framework for heterogeneous multiclass models with creeping. The porous model can allow a choice of two distinct velocity profiles for freeflow and restricted flow within each vehicle class, the specification of a time dependent distribution of pore spaces, and the function $s_{\max}(\cdot)$ (the maximum pore size and density relationship). The result is that porous model has potential to capture more complicated dynamics in highly heterogeneous flow.

However, significant analysis of the general porous model is missing, due in part to its increased flexibility/complexity. In contrast, the simpler creeping model is shown to be well-posed [18], which is important to guarantee that the discrete scheme (e.g., (20)) converges to the

admissible solution of the continuum model, and not an incorrect solution. In general, the well-posedness of heterogeneous multiclass models tends to be difficult to establish, as illustrated in the n–populations model [16].

The current paper proposed the discrete version of the creeping model. The accuracy of model needs to be determined with experimental data to assess the potential for use in traffic estimation and control applications. This can be done when traffic datasets that classify vehicle classes are available.

CONCLUSION

In this work, a discrete heterogeneous model for two vehicle classes is developed, which is based on a multiclass extension of the cell transmission model. The model is designed to model the creeping scenario when large vehicles are stopped, while smaller vehicles continue to move. To achieve this goal, velocity functions are introduced that have the same maximum velocity but distinct maximum occupied spaces. The model is described as a phase transition model where a 2×2 system of cell transmission models (in the non-creeping phase) reduces to the classical cell transmission model (in the creeping phase) as the occupied space increases above a critical point r_2^{m}. Finally, numerical tests are performed, and comparisons between the creeping mode, the two class n–populations model, and the porous model are carried out. These tests show that the creeping model and porous models can describe both overtaking, and the dynamics of creeping in heterogeneous flow. Moreover, compared with the stochastic porous model, the creeping model is deterministic and easier to implement.

ACKNOWLEDGMENTS

The first author would like to acknowledge funding provided by the California Department of Transportation under the PATH Connected Corridors program. The second author would like to acknowledge the support by the National Science Foundation under Grant No. 1351717.

References

[1] IBM, "The globalization of traffic congestion: IBM 2010 commuter pain survey." Website, 2010. `http://www-07.ibm.com/innovation/my/exhibit/documents/pdf/3_Globalization_of_Traffic.pdf`.

[2] M. J. Lighthill and G. B. Whitham, "On kinematic waves. II. A theory of traffic flow on long crowded roads," *Proc. Roy. Soc. A*, vol. 229, no. 1178, pp. 317–345, 1955.

[3] P. I. Richards, "Shock waves on the highway," *Oper. Res.*, vol. 4, pp. 42–51, 1956.

[4] B. D. Greenshields, "A study of traffic capacity," *Proc. of the Highway Research Record*, vol. 14, pp. 448–477, 1935.

[5] S. Smulders, "Control of freeway traffic flow by variable speed signs," *Transport. Res. B-Meth.*, vol. 24, no. 2, pp. 111 – 132, 1990.

[6] C. F. Daganzo, "The cell transmission model: A dynamic representation of highway traffic consistent with the hydrodynamic theory," *Transport. Res. B-Meth.*, vol. 28, pp. 269–287, 1994.

[7] S. K. Godunov, "A difference scheme for the numerical computation of a discontinuous solution of the hydrodynamic equations," *Math. Sbornik*, vol. 47, pp. 271–306, 1959.

[8] J. P. Lebacque, "The Godunov scheme and what it means for first order traffic flow models," in *13th International Symposium on Transportation and Traffic Theory*, pp. 647–677, 1996.

[9] S. Logghe and L. H. Immers, "Heterogeneous traffic flow modelling with the LWR model using passenger-car equivalents," in *Proc. of the 10th World Congress on ITS, Madrid (Spain)*, 2003.

[10] C. F. Daganzo, "A continuum theory of traffic dynamics for freeways with special lanes," *Transport. Res. B-Meth.*, vol. 31, no. 2, pp. 83–102, 1997.

[11] H. M. Zhang and W. L. Jin, "Kinematic wave traffic flow model for mixed traffic," *Transport. Res. Record*, vol. 1802, no. 1, pp. 197–204, 2002.

[12] D. Ngoduy and R. Liu, "Multiclass first-order simulation model to explain non-linear traffic phenomena," *Physica A*, vol. 385, no. 2, pp. 667–682, 2007.

[13] J. W. C. Van Lint, S. P. Hoogendoorn, and M. Schreuder, "Fastlane: New multiclass first-order traffic flow model," *Transport. Res. Record*, vol. 2088, no. 1, pp. 177–187, 2008.

[14] G. C. K. Wong and S. C. Wong, "A multi-class traffic flow modelï¿œ an extension of LWR model with heterogeneous drivers," *Transport. Res. A-Pol.*, vol. 36, no. 9, pp. 827 – 841, 2002.

[15] Z. Zhu and T. Wu, "Two-phase fluids model for freeway traffic flow and its application to simulate evolution of solitons in traffic," *J. Transp. Eng.*, vol. 129, no. 1, pp. 51–56, 2002.

[16] S. Benzoni-Gavage and R. M. Colombo, "An n-populations model for traffic flow," *Eur. J. Appl. Math.*, vol. 14, no. 5, pp. 587–612, 2003.

[17] R. Nair, H. S. Mahmassani, and E. Miller-Hooks, "A porous flow approach to modeling heterogeneous traffic in disordered systems," *Transport. Res. B-Meth.*, vol. 45, no. 9, pp. 1331 – 1345, 2011.

[18] S. Fan and D. Work, "A heterogeneous multiclass traffic flow model with creeping," 2014. `http://publish.illinois.edu/dbwork/publications/`.

[19] P. Zhang, R. X. Liu, S. C. Wong, and S. Q. Dai, "Hyperbolicity and kinematic waves of a class of multi-population partial differential equations," *Eur. J. Appl. Math.*, vol. 17, no. 2, pp. 171–200, 2006.

[20] S. Blandin, D. Work, P. Goatin, B. Piccoli, and A. Bayen, "A general phase transition model for vehicular traffic," *SIAM J. Appl. Math.*, vol. 71, no. 1, pp. 107–127, 2011.

[21] R. M. Colombo, "Hyperbolic phase transitions in traffic flow," *SIAM J. Appl. Math.*, vol. 63, pp. 708–721, 2003.

[22] S. Fan and B. Seibold, "A comparison of data-fitted first order traffic models and their second order generalizations via trajectory and sensor data," Transport. Res. Board, (Washington DC), 2013. paper number 13–4853.

[23] J. Glimm, "Solutions in the large for nonlinear hyperbolic systems of equations," *Comm. Pure Appl. Math.*, vol. 18, no. 4, pp. 697–715, 1965.

[24] T. P. Liu and T. Yang, "Weak solutions of general systems of hyperbolic conservation laws," *Commun. Math. Phys.*, vol. 230, no. 2, pp. 289–327, 2002.

[25] F. Ancona and A. Marson, "Existence theory by front tracking for general nonlinear hyperbolic systems," *Arch. Ration. Mech. An.*, vol. 185, no. 2, pp. 287–340, 2007.

[26] A. Bressan, *Hyperbolic systems of conservation laws – The one dimensional Cauchy problem*. Oxford: Oxford University Press, 2000.